

Specific-Heat Exponent of Random-Field Systems via Ground-State Calculations

A.K. Hartmann* and A.P. Young†

Department of Physics, University of California, Santa Cruz CA 95064, USA

(October 30, 2018)

Exact ground states of three-dimensional random field Ising magnets (RFIM) with Gaussian distribution of the disorder are calculated using graph-theoretical algorithms. Systems for different strengths h of the random fields and sizes up to $N = 96^3$ are considered. By numerically differentiating the bond-energy with respect to h a specific-heat like quantity is obtained, which does not appear to diverge at the critical point but rather exhibits a cusp. We also consider the effect of a small uniform magnetic field, which allows us to calculate the $T = 0$ susceptibility. From a finite-size scaling analysis, we obtain the critical exponents $\nu = 1.32(7)$, $\alpha = -0.63(7)$, $\eta = 0.50(3)$ and find that the critical strength of the random field is $h_c = 2.28(1)$. We discuss the significance of the result that α appears to be strongly negative.

PACS numbers: 75.50.Lk, 05.70.Jk, 75.40.Mg, 77.80.Bh

I. INTRODUCTION

The random field Ising model [1] has been extensively studied [2–4] both because of its interest as a “simple” frustrated system and because of its relevance to experiments, especially those on the diluted antiferromagnet in a uniform field [5]. The RFIM Hamiltonian is given by

$$\mathcal{H} = -J \sum_{\langle i,j \rangle} S_i S_j - \sum_i h_i S_i, \quad (1)$$

where the $S_i = \pm 1$ are Ising spins, J is the interaction energy between nearest neighbors, and h_i is the random field. The values h_i are independently distributed according a Gaussian distribution with mean 0 and standard deviation h , i.e. the probability distribution is

$$P(h_i) = \frac{1}{\sqrt{2\pi}h} \exp\left(-\frac{h_i^2}{2h^2}\right). \quad (2)$$

We shall consider three-dimensional lattices with periodic boundary condition and $N = L^3$ spins.

A sketch of the phase boundary is shown in Fig. 1. At low values of the random field and temperature T , the system is in a ferromagnetic phase, and at high temperatures or random fields, the system is paramagnetic.

In this paper we shall be interested in the values of the critical exponents along the phase boundary. The random field is a relevant perturbation at the pure (i.e. $h = 0$) fixed point, and the random-field fixed point is at $T = 0$ [6,7]. Hence, the critical behavior is the same everywhere along the phase boundary in Fig. 1 (assuming that the transition is always second order) except for $h = 0$. We can therefore determine the critical behavior by staying at $T = 0$ and crossing the phase boundary at $h = h_c$, see Fig. 1, which is convenient, because we can determine the ground states of large lattices exactly using efficient optimization algorithms [8–11], as discussed in Sec. II. This has the advantage that one can study much larger systems than it is possible in Monte Carlo simulations, and, for each realization, there are no statistical errors or equilibration problems.

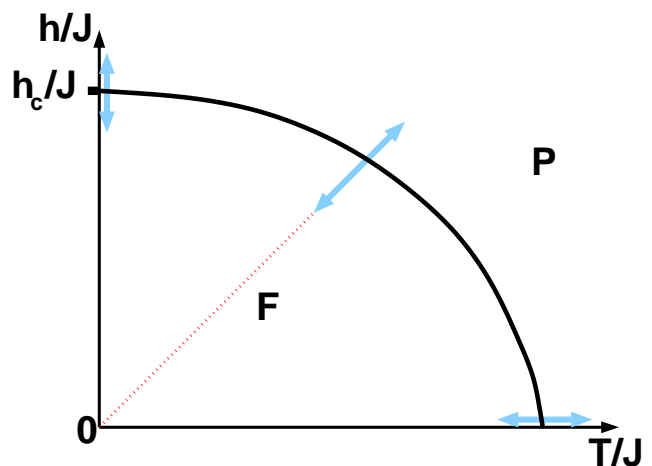


FIG. 1. A sketch of the phase boundary of the random field Ising model. The ferromagnetic phase is denoted by “F” and the paramagnetic phase by “P”. The critical value of the random field at $T = 0$ is denoted by h_c . The lines with arrows at both ends indicate the path followed by varying J for some fixed value of h and T .

Using these ground state techniques, most of the critical exponents have been determined with some precision; for a thorough recent study see Ref. [12]. Most of these exponents are consistent with scaling relations. However, as we shall discuss in Sec. V, those scaling relations predict a specific-heat exponent α close to zero, while Monte Carlo data on fairly small sizes [13] ($L \leq 16$) find $\alpha/\nu = -0.45 \pm 0.05$, where ν is the correlation length exponent (which has a value slightly greater than unity, as discussed in Secs. IV and V). Interestingly, experiments find [14] a logarithmic divergence, corresponding to a specific heat exponent $\alpha = 0$, as expected from scaling.

In order to try to resolve this puzzle, we calculate here the specific heat exponent for the RFIM using *much* larger sizes ($L \leq 96$) than in the Monte Carlo work

[13], by using optimization methods to determine exact ground states. We also find a strongly negative value for α , $\alpha/\nu = -0.48 \pm 0.05$, consistent with the earlier Monte Carlo data [13], but in disagreement with experiment and apparently in violation of scaling. In Sec. V we will discuss possible ways round this discrepancy. In addition, we determine the susceptibility, which, to our knowledge, has not been directly computed before using ground-state methods. Our results are consistent with earlier calculations.

II. NUMERICAL TECHNIQUES

We used well known algorithms [8–11] from graph theory [15–17] to calculate the ground state of a system at given random-field strength h . To implement them we applied some algorithms from the LEDA library [18]. The calculation works by transforming the system into a network [19], and calculating the maximum flow in polynomial time [20–24]. The first results of applying these algorithms to random-field systems can be found in Ref. [25]. In Ref. [26] these methods were applied to obtain the exponents for the magnetization, the disconnected susceptibility and the correlation length from ground-state calculations up to size $L = 80$. Other exact ground-state calculation of the RFIM can be found in Refs. [27–29,12]. Note that in cases where the ground-state is degenerate [30] it is possible to calculate all the ground-states in one sweep [31], see also Refs. [32,33]. For the RFIM with a Gaussian distribution of fields, the ground state is non-degenerate, except for a two-fold degeneracy at certain values of the randomness, where the ground state changes, see Sec. III, so it is sufficient to calculate just one ground state.

III. QUANTITIES OF INTEREST

In zero random field, the specific-heat exponent is obtained from the singularity in the second derivative of the free energy with respect to temperature. More generally it is determined from the singularity obtained by varying a parameter which crosses the phase boundary from the paramagnetic phase to the ferromagnetic phase. From Fig. 1 we see that this can be conveniently accomplished by keeping the ratio of h/J to T/J fixed, i.e. by varying J . The first derivative of the free energy (per spin) F with respect to J , which we call the “bond energy” E_J , is given by

$$E_J \equiv \frac{\partial F}{\partial J} = -\frac{1}{N} \sum_{\langle i,j \rangle} \langle S_i S_j \rangle, \quad (3)$$

where $\langle \dots \rangle$ is a thermal average, and the sum is over nearest-neighbor pairs. E_J has an energy-like singularity in the vicinity of the phase boundary. For $h = 0$ it is *precisely* the energy, apart from an overall factor of J .

The total energy per spin, E , is given by

$$E = JE_J + hE_h, \quad (4)$$

where the “field energy” E_h is given by

$$E_h \equiv \frac{\partial F}{\partial h} = -\frac{1}{N} \sum_i \left(\frac{h_i}{h} \right) \langle S_i \rangle. \quad (5)$$

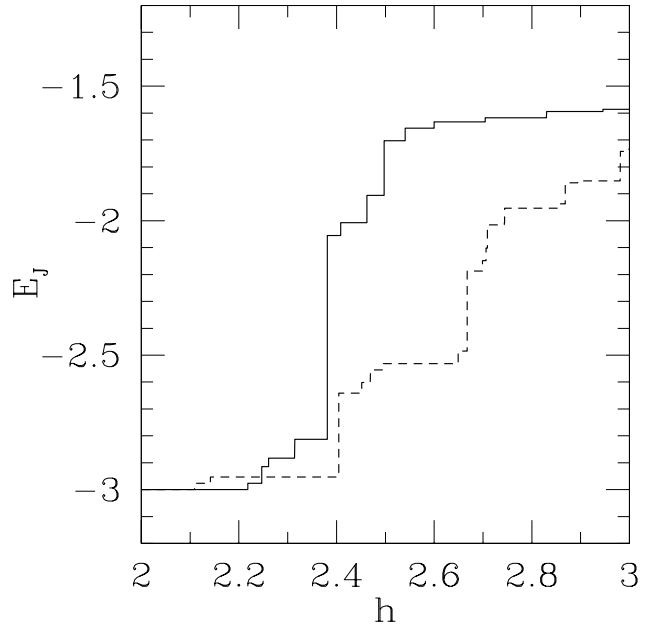


FIG. 2. Bond energy per spin, E_J , defined in Eq. (3), for two $L = 8$ samples as a function of the random-field strength h .

Having differentiated *analytically* with respect to J , we now set $J = 1$, consider $T = 0$ only, and obtain a specific heat-like quantity by differentiating E_J *numerically* with respect to the random field h . We emphasize that it is not necessary to vary the temperature in order to observe the specific heat singularity. To observe this singularity the direction in which the phase boundary is crossed must have a projection on to the correct scaling field, which means that the phase boundary should not be approached tangentially. The angle at which the phase boundary is approached will affect the size of *corrections* to scaling by mixing in a varying amount of irrelevant operators, but the asymptotic behavior will always be the same (as long as the approach is not tangential).

To avoid confusion we point out that the role taken by the free energy at finite- T is played by the energy at $T = 0$, since the two are equal in this limit. More precisely, the *energy* singularity at $T = 0$ has the form $\epsilon^{2-\alpha}$, where ϵ is the deviation from criticality, which is the same as the *free-energy* singularity at a finite- T transition. At finite- T , the energy and entropy each have a

stronger singularity, of the form $\epsilon^{1-\alpha}$, but with opposite signs such that this singularity cancels in the free energy, $F = E - TS$. A analogous cancellation occurs at $T = 0$, but between E_J and E_h since both E_J and E_h have singularities with exponent $1 - \alpha$ but with amplitudes of opposite sign such that this singularity cancels in the total energy. To see this note that from Eq. (4)

$$\frac{\partial E}{\partial h} = J \frac{\partial E_J}{\partial h} + h \frac{\partial E_h}{\partial h} + E_h. \quad (6)$$

However, at $T = 0$ where $F = E$, we have $\partial E/\partial h = E_h$, and so, in this limit,

$$J \frac{\partial E_J}{\partial h} + h \frac{\partial E_h}{\partial h} = 0. \quad (7)$$

Hence, if $E_h \sim |h - h_c|^{1-\alpha}$, then $\partial E_h/\partial h$ and $\partial E_J/\partial h$ each have singularities of the form $|h - h_c|^{-\alpha}$, but with opposite signs such that this singularity cancels in $\partial E/\partial h$. We have verified that this cancellation occurs in our numerical data. From Eqs. (6) and (7), $\partial E/\partial h$ has the same singularity as E_h , i.e. $|h - h_c|^{1-\alpha}$, so $E \sim |h - h_c|^{2-\alpha}$, as stated above.

We use the same set of random fields for different values of h and scale them all by a fixed overall factor. More precisely we take $h_i = \epsilon_i h$, where the ϵ_i are chosen from a Gaussian distribution with standard deviation *unity*, and are the same [34] for all values of h . We use a first-order finite difference to determine the derivative of E_J numerically and, since this is a more accurate representation of the derivative at the midpoint of the interval than at either endpoint, the “specific heat”, C , at $T = 0$ is defined to be

$$C \left(\frac{h_1 + h_2}{2} \right) = \frac{[E_J(h_1)]_h - [E_J(h_2)]_h}{h_1 - h_2}, \quad (8)$$

where h_1 and h_2 are two “close-by” values of h , and $[\cdot]_h$ denotes an average over random-field configurations, which is carried out (approximately) by repeating the calculation for N_{samp} independent realizations (samples) of the random fields ϵ_i . We choose a sufficiently fine mesh of random-field values that the resulting data for C is smooth. Error bars are obtained by determining the specific heat from the corresponding finite difference as in Eq. (8) for each sample separately, and computing the standard deviation. The error bar is, as usual, the standard deviation divided by $\sqrt{N_{\text{samp}} - 1}$.

In Fig. 2 the bond energy per spin E_J for two representative $L = 8$ systems is shown as a function of h . For very small values of h all spins point into the same direction and so $E_J = -3$. For large h the spins follow the random fields and so $E_J \rightarrow 0$ in this limit. The curves in Fig. 2 are stepwise constant functions because generically it is not favorable to flip spins if the random field is increased by a small amount. However, at certain discrete field values, the total energy of another state, which differs in the orientation of a cluster of spins, will

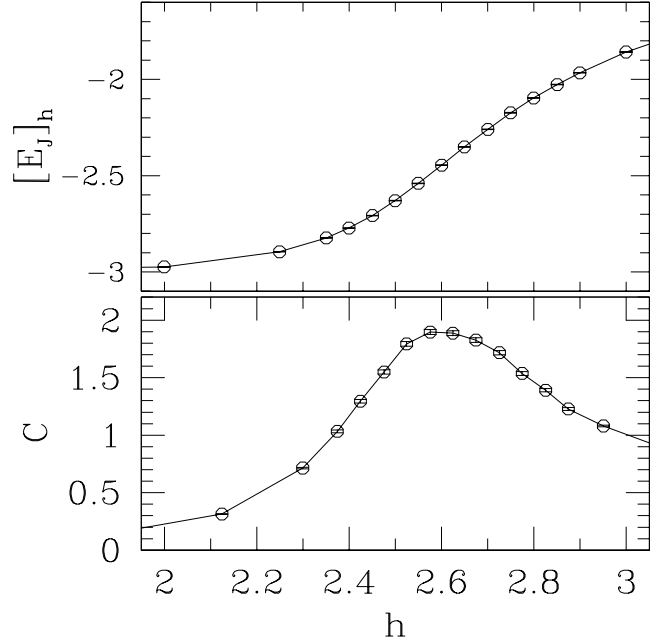


FIG. 3. The upper figure shows the average bond-energy $[E_J]_h$ per spin as a function a function of the random-field strength h for $L = 16$. The lower figure displays the resulting “specific heat”, calculated from Eq. (8) of the text.

become degenerate with the energy of the ground state and for slightly larger values of h the state with the cluster flipped will become the new ground state. Although the *total* energy is continuous at the field values where the ground state configuration changes, the bond energy, which is just the first term in Eq. (1), changes discontinuously. At larger field values the jumps in E_J occur closer together and would be difficult to distinguish on the scale of a figure. This is why we show, in Fig. 3, data for a rather small size. Even for small sizes, the jumps occur at different values of h for different samples, and so the *average* value of E_J is expected to be smooth.

This is illustrated in the upper part of Fig. 3 for $L = 16$ which shows a smooth variation of $[E_J]_h$ with h . The data in the lower part of the figure is the average specific heat, obtained as the numerical derivative of the data for $[E_J]_h$ according to Eq. (8). The specific heat is seen to have a peak, as expected. We will investigate the size dependence of this peak in Sec. IV.

In addition to the specific heat, we also calculate the susceptibility by considering the response to a small uniform external field H , i.e. we consider the Hamiltonian

$$\mathcal{H} = -J \sum_{\langle i,j \rangle} S_i S_j - \sum_i h_i S_i - H \sum_i S_i. \quad (9)$$

For each realization, the sign of H is chosen in the direction of the magnetization of the ground state. This prevents the whole system from flipping when applying a

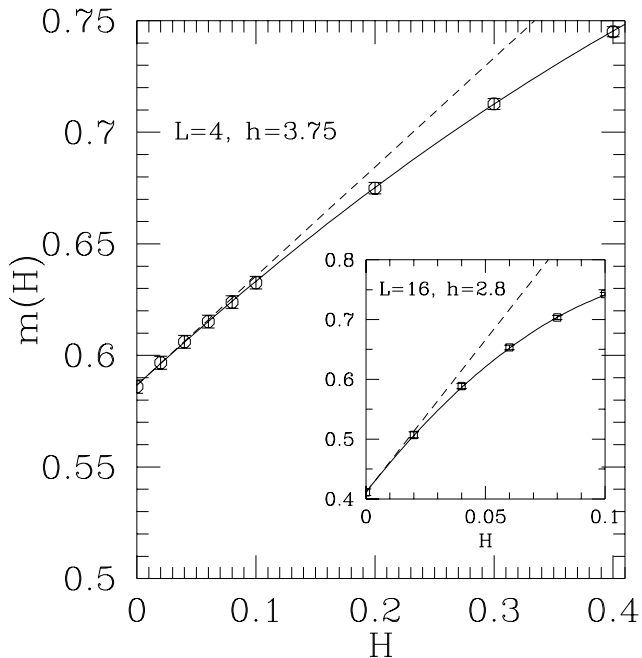


FIG. 4. The average magnetization m as a function of a uniform external field H near the transition for $L = 4, h = 3.75$ (inset: $L = 16, h = 2.8$). The solid lines represent the results of fits to a parabola, while the dashed lines display the tangents at $H = 0$; i.e. their slope gives the susceptibility.

magnetic field to a system which is almost ferromagnetically ordered. The scaling behavior of the magnetization should not be affected by this choice. In Fig. 4, the result is shown for system sizes $L = 4$ and $L = 16$ near the values of the field, where the susceptibility attains a maximum. Near $H = 0$, the data points can be fitted very well with a parabola, the coefficient of the linear term gives the zero field susceptibility $\chi = dm/dH|_{H=0}$. Thus, in order to calculate the susceptibilities, we perform ground state calculations for three different values of the uniform field $H_n = nH_L$ ($n = 0, 1, 2$), where, for each size, the value of H_L used is shown in Table. I, along with the number of samples. We chose the values of H_L for each size as follows. For the smaller sizes we performed several fields values, as shown in Fig. 4, to determine for what range of fields a parabola accurately fitted the data. For larger sizes, finite-size scaling tells us that, near the critical point, the characteristic field scales with L as L^{-y_H} where the “magnetic exponent” y_H is given by $(\gamma + \beta)/\nu$, with γ the susceptibility exponent, and β the order parameter exponent. As discussed further in Sec. V, several calculations give $\beta \simeq 0, \gamma \simeq 2$, and $\nu \simeq 1.3$, and so $y_H \simeq 1.5$. We therefore scale H_L for the larger sizes by a factor of roughly $L^{-1.5}$.

For each system size, we fit a parabola through the three data points for the *average* magnetization $m(H_n)$. To estimate the error, we performed a jackknife analysis [35] in which we divided the results for the magnetizations (for each system size and each strength of the disorder) into K blocks, calculated the average values K times, each time omitting one of the blocks, and then performing K fits. The error bar is estimated from the variance of the K results for the linear fitting parameter. We used $K = 50$ and checked that the result does not depend much on the choice of K .

L	N_{samp}	H_L
4	10^5	0.05
6	60000	0.025
8	40000	0.016
12	30000	0.008
16	23000	0.005
24	27000	0.0028
32	15000	0.0018
48	15000	9×10^{-4}
64	9000	6×10^{-4}
96	3800	3×10^{-4}

TABLE I. The maximum number of samples N_{samp} used, and sizes of smallest non-zero uniform field H_L , for each system size L . As discussed in the text, the number of samples used was larger in the vicinity of the peaks in the susceptibility and specific heat than elsewhere.

IV. RESULTS

We have studied random-field systems with sizes from $L = 4$ to $L = 96$. For each size, simulations were made for several different values of h , always averaged over many realizations of the disorder. Near the ferromagnet-paramagnet phase transition, the number of samples used is the largest, ranging from 10^5 for the smaller system sizes to 3800 for $L = 96$ for each value h , as shown in Table I. With current algorithms, it is in principle possible to study even larger system sizes, such as $L = 128$ or even $L = 256$, but, using the LEDA algorithms, these need more memory than the 512 MBytes available to us. Hence we have restricted our study to $L \leq 96$, which is still much larger than sizes that can be simulated using Monte Carlo simulations.

In the thermodynamic limit *the singular part of the specific heat diverges according to*

$$C_s \approx A_{\pm} |h - h_c|^{-\alpha}, \quad (10)$$

where the *amplitudes* A_+ and A_- refer to $h > h_c$ and $h < h_c$ respectively, and α is the specific heat exponent. In addition there is a *regular* piece of the specific heat, C_{reg} , which is finite at the critical point and so *dominates* there if $\alpha < 0$. In a finite system, finite-size scaling predicts that

$$C_s \sim L^{\alpha/\nu} \tilde{C} \left((h - h_c) L^{1/\nu} \right), \quad (11)$$

where ν is the correlation length exponent. The specific heat peak will occur when the argument of the scaling function \tilde{C} takes some value, a_1 say, so the peak position $h^*(L)$ varies as

$$h^*(L) - h_c \approx a_1 L^{-1/\nu}, \quad (12)$$

and the value of the singular part of the specific heat at the peak varies as

$$C_s^{\text{max}}(L) \sim L^{\alpha/\nu}. \quad (13)$$

In Fig. 5 the specific heat C is shown as a function of the random-field strength h for selected system sizes. The error bars are obtained from the standard deviation of the data for different samples, and are quite small because a large number of samples have been averaged over, see Table I. A clear peak can be seen, which moves to the left and increases in height with increasing system size. The number of samples used is larger near the peak to compensate for the greater sample to sample fluctuations in this region. For each system size, we performed parabolic fits to the region of the peak to obtain $h^*(L)$ and the height of the peak, $C^{\text{max}}(L)$. The shift of the maximum according to Eq. (12) can be used to estimate the infinite-size critical strength of the random field, h_c and the correlation-length exponent ν . The best fit gives

$$h_c = 2.28 \pm 0.01, \quad 1/\nu = 0.73 \pm 0.02, \quad (14)$$

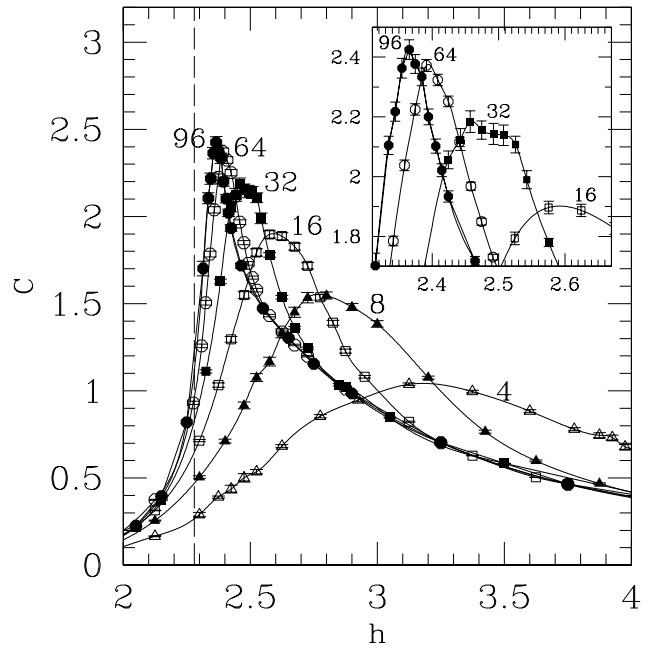


FIG. 5. “Specific heat” C , calculated from Eq. (8), as a function of the random-field strength h for system sizes $L = 4, 8, 16, 32, 64$ and 96 . The vertical dashed line indicates the location of the critical value of the random field, $h_c = 2.28$, see Eq. (14). The inset is an enlargement of the peaks for the larger sizes.

see Fig. 6. We determined the probability Q that the value of $\chi^2 = \sum_{i=1}^N \left(\frac{y_i - f(x_i)}{\sigma_i} \right)^2$, with N data points $(x_i, y_i \pm \sigma_i)$ fitted to the function f , is worse than in the current fit [36] to quantify the quality of the fit. Here we get $Q = 0.20$, which is fair.

Next we try to estimate the specific heat exponent by looking at how the peak value C^{max} scales with L . If $\alpha = 0$ one expects logarithmic divergence and the simplest hypothesis is to fit the data to

$$C^{\text{max}} = a + b \log L, \quad (15)$$

where the constant term a comes partly from the regular piece of the specific heat. However, Fig. 7 shows that this does not work. A plot of C^{max} against L (on a log scale) shows clear curvature, suggesting that the height of the specific heat will saturate to a finite value as L increases. If one considers only the data points for sizes $L = 4, \dots, 16$, as in Ref. [13], a negative curvature is still visible, but the result is much less clear.

A peak height which saturates for $L \rightarrow \infty$ implies that α is negative, in which case the specific heat has a finite cusp at the critical point, rather than a divergence. We have therefore tried a fit of the form

$$C^{\text{max}}(L) = C_{\infty} + a_2 L^{\alpha/\nu}, \quad (16)$$

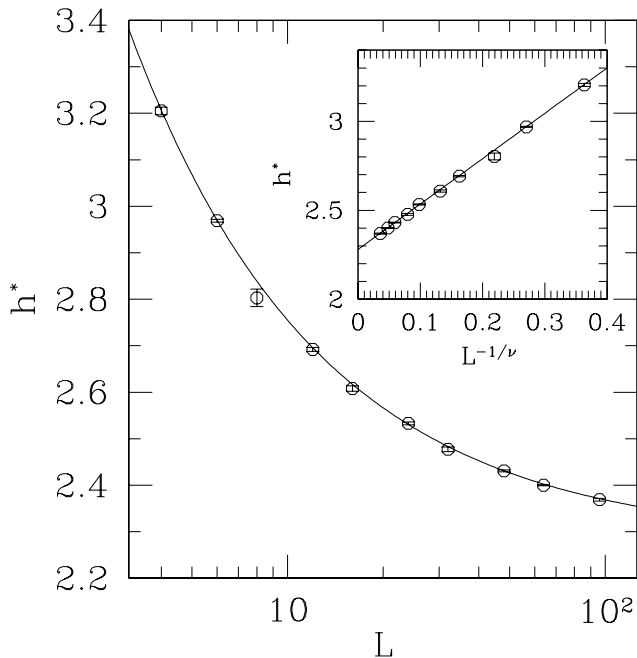


FIG. 6. A plot of the random field where the specific heat attains its maximum, as a function of system size L . The solid line shows a fit to the function $h^*(L) = h_c + a_1 L^{-1/\nu}$ with $h_c = 2.28$, $1/\nu = 0.73$, and $a_1 = 2.55$. The inset shows the data as a function of $L^{-1/\nu}$.

in which C_∞ comes from the regular part of the specific heat, yielding,

$$c_\infty = 2.84 \pm 0.05, \quad \alpha/\nu = -0.48 \pm 0.03. \quad (17)$$

This fit is shown in the inset of Fig. 7. The quality of the fit, $Q = 0.05$, is not very good. We have tried different fits using only the larger system sizes, which increases the quality of the fit slightly, but the resulting error bars are very large. The central estimate for α actually becomes *more negative* if we only include the larger sizes. The rather poor fit may indicate difficulty in accurately estimating the error bars for the location and height of the specific heat peak. Our analysis suggests that the specific heat exponent is strongly negative, in agreement with Rieger [13] though we cannot rule out a leading singularity with $\alpha \simeq 0$ and a sufficiently small amplitude that it is hard to see in our data.

To look for this possibility, we also tried more complicated fits including corrections to scaling of the form

$$C^{\max}(L) = C_\infty + a_2 L^{\alpha/\nu} (1 + bL^{-\omega}), \quad (18)$$

where ω is the leading correction to scaling exponent. The data did not determine all the parameters cleanly, and the fit program [37], which works iteratively, converged to different results depending on the starting values, and whether any of the parameters were held fixed.

The solutions we found were of two types: (i) the fit is the same as that in the simpler fit of Eq. (16) (i.e. ω is essentially zero and α/ν and the other parameters are the same as found in the simpler fit), (ii) ω is quite small, a_2 is very large, and b is negative such that $1 + bL^{-\omega}$ is close to zero. Thus, in the second type of fit, the data is represented as two singularities with large amplitudes which almost cancel. This does not seem physical. The fitting routine did not converge to a solution with a leading singularity which has a small amplitude and $\alpha \simeq 0$, plus a correction term with a larger amplitude.

We will discuss our specific heat results further in Sec. V.

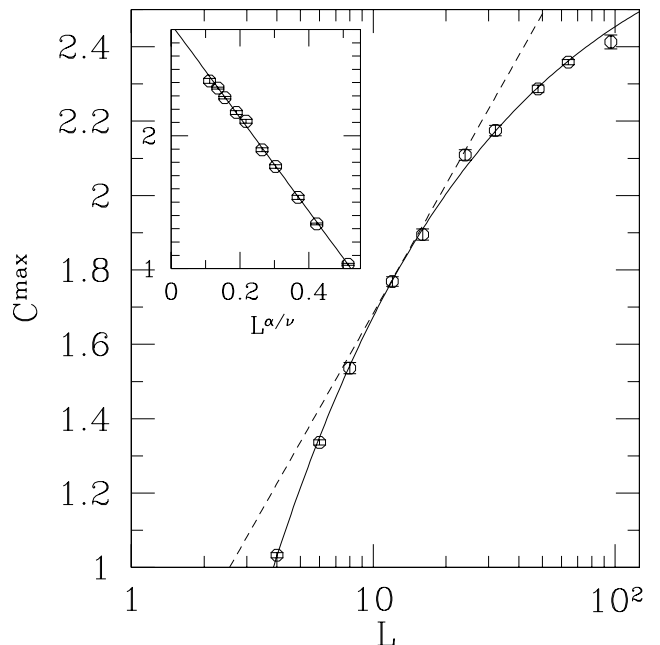


FIG. 7. The maximum C^{\max} of the specific heat as a function of system size L with logarithmically scaled L -axis. The dashed line is a tangent to the data and a comparison between it and the data demonstrates that C^{\max} grows slower than logarithmically with system size. The solid line shows a fit to the function $C^{\max}(L) = C_\infty + a_2 L^{\alpha/\nu}$ with $C_\infty = 2.84$, $\alpha/\nu = -0.48$ and $a_2 = -3.52$. The inset shows the data and the fit as a function of $L^{\alpha/\nu}$.

The susceptibility χ as a function of h is presented in Fig. 8 for selected system sizes. It is seen that the height of the peak grows much faster than for the specific heat. To analyze the divergence of χ , we have again fitted parabolas to the data points near the peak to obtain the positions $h^*(L)$ and $\chi^{\max}(L)$ of the maximum. By fitting the data for $L \geq 32$ to a function $\chi^{\max}(L) = a_3 L^{2-\eta}$, where η describes the decay of the “connected” correlations at criticality, we obtain ($Q = 0.63$)

$$\eta = 0.50 \pm 0.03, \quad (19)$$

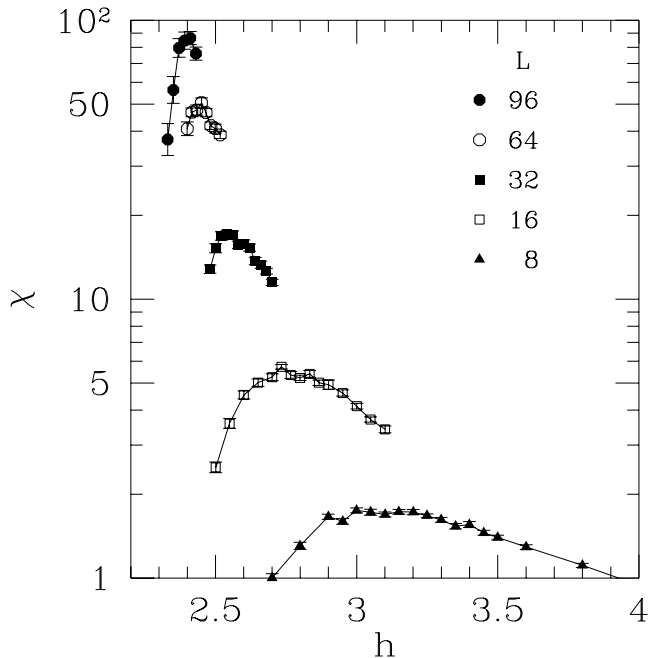


FIG. 8. Susceptibility χ as a function of the random-field strength h for system sizes $L = 8, 16, 32, 64,$ and 96 . Only data near the peaks is shown because the data away from the peaks had lower precision.

see Fig. 9.

Finally, we have also estimated h_c and the correlation-length exponent from the susceptibility data using Eq. (12), as we did for the specific heat. Using only sizes $L \geq 32$ ($Q = 0.84$), we find

$$h_c = 2.29 \pm 0.01, \quad 1/\nu = 0.81 \pm 0.05. \quad (20)$$

This estimate of h_c agrees with that obtained from the specific heat, see Eq. (14), while the estimate for $1/\nu$ differs from that in Eq. (14) by slightly more than the sum of the error bars, probably indicating some systematic corrections to scaling.

V. DISCUSSION

We have determined the “specific heat” of the random field Ising model at $T = 0$ using optimization algorithms. The height of the peak increases less fast than logarithmically with system size, and a finite-size scaling analysis gives the exponents shown in Eqs. (14) and (17). From the analysis of the susceptibility, the exponents shown in Eqs. (19) and (20) are obtained. The final results we quote are

$$\begin{aligned} h_c &= 2.28 \pm 0.01, \quad \nu = 1.32 \pm 0.07 \\ \alpha &= -0.63 \pm 0.07, \quad \eta = 0.50 \pm 0.03. \end{aligned} \quad (21)$$

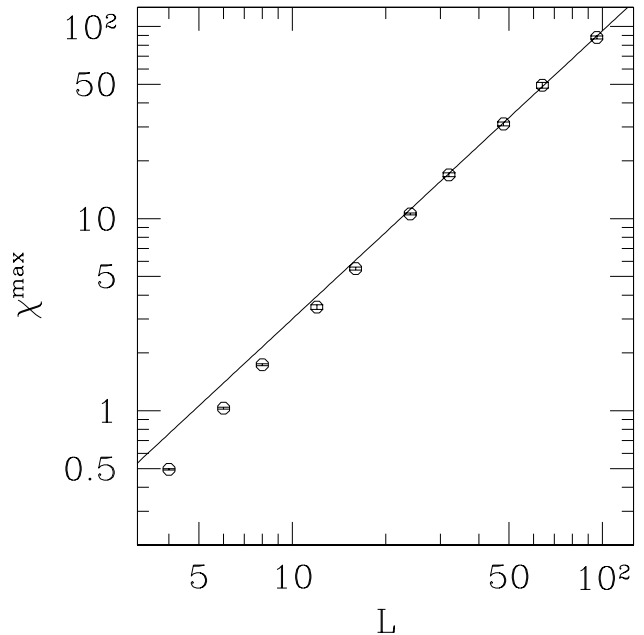


FIG. 9. The maximum χ^{\max} of the susceptibility as a function of system size L in a double logarithmic plot. The solid line represents a fit to the function $\chi^{\max}(L) = a_3 L^{2-\eta}$, for sizes $L \geq 32$ yielding $2 - \eta = 1.50$ and $a_3 = 0.095$.

To determine ν and its error we have taken both the values in Eqs. (14) and (20) and used the difference between them as a measure of the systematic error. The errors for η and h_c are purely statistical. The error for α comes both from the error in ν and the statistical error in α/ν .

Our results for h_c are compatible with the values 2.29 ± 0.04 [26], 2.26 ± 0.01 [27], and 2.270 ± 0.005 [12] obtained from ground-state calculations of systems of similar size. Values of ν obtained from ground-state calculations are 1.37 ± 0.09 [12] and 1.19 ± 0.08 , [26], which agree well with our result. Ref. [27] argued for a first-order transition, but assuming scaling with respect to the field, a value of $\nu = 1.25 \pm 0.06$ was estimated, also in agreement with our result. However, if a power law correction to scaling was taken into account, instead the result 1.52 (without error bars) was found.

The scaling exponent η describing the susceptibility, has not been obtained from exact ground-state calculations so far. In a Monte-Carlo simulation [13] a value of 0.50 ± 0.05 was found, which is compatible with our result.

The most significant result of this paper is that for the specific heat, namely $\alpha = -0.63(7)$. This agrees well with the values $\alpha/\nu = -0.45 \pm 0.05$, $\nu = 1.1 \pm 0.2$ found by Ref. [13] and $\alpha = -0.55 \pm 0.20$ found by Ref. [29], both using Monte Carlo simulations on small systems. However, as we shall now see, it appears inconsistent with values for other exponents and expected scaling relations.

At conventional second-order phase transitions, all exponents can be related to *two* (e.g. ν and η) by scaling relations. However, because the fixed point of the RFIM is at $T = 0$ with temperature a “dangerous irrelevant variable”, a modified set of scaling relations has been proposed [6,7,38,39], which involve *three* independent exponents. Scaling relations which do not involve the space dimension, e.g.

$$\alpha + 2\beta + \gamma = 2, \quad (22)$$

are unchanged, but “hyperscaling” relations involving the space dimension d , have d replaced by $d - \theta$, where θ , the third exponent, is the scaling exponent for the temperature at the fixed point. An example of a hyperscaling relation which is relevant to the specific heat is

$$(d - \theta)\nu = 2 - \alpha. \quad (23)$$

Gofman et al. [40] have proposed that the Schwartz-Soffer [41] inequality, which can be expressed as $\eta \geq 2 - \theta$, is an equality, in which case there are only two independent exponents again (though the hyperscaling relations are different from those in conventional two-exponent scaling). Our results are consistent with this, since $\beta \simeq 0$ implies that $\theta \simeq 1.5$, see e.g. Ref. [12], and we have already found that η is about 0.50, see Eq. (19).

Other works have found [13,26] $\beta \simeq 0$ (the most accurate value is 0.017 ± 0.005 in Ref. [12]), and our value for γ , obtained from $\gamma \equiv (2 - \eta)\nu$ is about 2.0 in agreement with series expansion work of Gofman et al. [40]. Hence Eq. (22) predicts $\alpha \simeq 0$, quite different from the value of about -0.63 that we find by direct calculation.

As noted above, the result $\beta \simeq 0$ implies that $\theta \simeq 1.5$, so Eq. (23) gives $\alpha \simeq 2 - 1.5\nu$. Using our value of $\nu = 1.32 \pm 0.07$ this yields $\alpha = 0.0 \pm 0.15$. In other words, Eq. (23) also predicts that α is close to zero.

We have seen that the two scaling relations above would be consistent if we inserted $\alpha \simeq 0$, which is the experimental value [14]. However, by direct calculation, we obtain a strongly negative result, $\alpha \simeq -0.63$, consistent with earlier work [13] on much smaller sizes. Thus the problem with the value of the specific-heat exponent has now been strongly reinforced by our calculations on much larger lattices.

Possible explanations for this discrepancy are:

- The specific heat diverges but slower than logarithmically. Examples of this, which are known to occur in other systems, are a fractional power of a log and a log-log variation. However, there are no calculations which predict this type of behavior for the RFIM. Furthermore, attempts to fit our data to this type of behavior were not very successful. A related possibility, which does not seem impossible looking at Fig. 5, is that $\alpha = 0$ might be realized by a *jump* in the specific heat, with a lower value in the ferromagnetic region, the opposite of what occurs in mean field theory.

- The regular contribution to the specific heat varies rapidly near the critical point. Since $\beta \simeq 0$ the magnetization increases very rapidly below h_c (leading to the very rapid drop in the specific heat seen in Fig. 5). If much of this drop comes from the regular part of the specific heat it would be difficult to extract the singular part.
- There are very strong singular corrections to finite-size scaling which leads to the most singular term in the specific heat being numerically small compared with correction terms, even for the quite large range of sizes that we have studied here. If there *are* strong corrections to scaling, perhaps the values of other exponents, in addition to α , could be affected too.
- Scaling does not hold. We find this possibility to be the least palatable.

Since $\beta \simeq 0$, it is interesting to ask whether the transition might be first order and whether this might be the origin of the surprising value of α . The transition at low- T is first order in mean field theory for field distributions with a minimum at zero field [42]. A first order transition for Gaussian distribution has also been suggested for dimension less than four based on series expansion work [43]. If the transition is first order, it must be very weakly so, since fluctuation effects are very large. Furthermore, one would then expect a latent heat, which, in a finite-size system, gives a specific heat diverging as the volume L^d . In our results, we do not see *any* divergence, let alone a strong one like this. In addition, the most detailed numerical study [12] claims that β while very small, is *greater* than zero. Even if the transition were ultimately first order, the effective exponents found should be those of the close-by second order transition, and so should satisfy scaling. We therefore don’t feel that the possibility of a first order transition explains why our value for α does not satisfy scaling.

In addition to critical exponents, it is useful to discuss amplitude ratios, since these are also universal, see Ref. [44] and references therein. For the specific heat amplitudes, A_+ and A_- , defined in Eq. (10), one can show [45] that $A_+/A_- = 1$ for a logarithmic divergence ($\alpha = 0$). Furthermore, for n -component models without random fields one has [44,46] $A_+/A_- > 1$ for $\alpha < 0$ and $A_+/A_- < 1$ if $\alpha > 0$. This implies that, for both signs of α , the specific heat decreases from its peak faster on the paramagnetic side than on the ferromagnetic side (we are grateful to D. Belanger for pointing this out). By contrast, the situation is reversed in our data, see Fig. 5 where the specific heat appears to decrease faster for $h < h_c$. Whether this indicates that the amplitude ratio is very different in the presence of random fields, or that corrections to scaling are large compared with the leading singularity for this range of sizes remains to be seen.

Clearly more work is needed to understand the specific heat of the RFIM. Since several recent large-scale numerical calculations, including ours, have used fairly sophisticated algorithms, it is unlikely that a numerical breakthrough is imminent. Hence a better theoretical understanding, especially of corrections to scaling, will be needed to sort out this problem.

Additional Note: After this work was submitted we received the final version [47] of Ref. [12] in which, motivated by our work, they computed the bond energy using ground state methods. They did not numerically differentiate the data to get the specific heat but directly analyzed data for the bond energy at the bulk critical field, the dashed line in Fig. 5. The size dependence involves the exponent $(1-\alpha)/\nu$ from which they find results compatible with $\alpha = 0$. That they get a different result from ours by, in effect, considering a different region of the scaling function in Eq. (11), indicates that there are large corrections to finite size scaling even for such large sizes, or possibly that $\alpha \simeq 0$ corresponds to a discontinuity in the specific heat. Both these possibilities were discussed above. Further work is needed to clarify the situation.

ACKNOWLEDGMENTS

We thank D. P. Belanger for stimulating discussions and Alan Middleton for giving helpful hints, showing us an advance copy of Ref. [12], and commenting on an earlier version of this paper. The simulations were performed at the Paderborn Center for Parallel Computing in Germany and on a workstation cluster at the Institut für Theoretische Physik, University of Göttingen, Germany. AKH acknowledges financial support from the DFG (Deutsche Forschungsgemeinschaft) under grant Ha 3169/1-1. APY acknowledges support from the NSF through grant DMR 0086287.

* hartmann@bach.ucsc.edu

† peter@bartok.ucsc.edu

[1] Y. Imry and S.-K. Ma, Phys. Rev. Lett. **35**, 1399 (1975).
 [2] D. P. Belanger and A. P. Young, J. Magn. and Magn. Mat. **100**, 272 (1991).
 [3] H. Rieger, in: *Annual Reviews of Computational Physics II* (ed. D. Stauffer), 295-341, World Scientific, Singapore 1995.
 [4] See e.g. the articles by D. P. Belanger and T. Nattermann in *Spin Glasses and Random Fields*, A. P. Young (Ed.), World Scientific, 1998.
 [5] S. Fishman and A. Aharony, J. Phys. C, **12**, L729 (1979).
 [6] A. J. Bray and M. A. Moore, J. Phys. C **18** L927 (1985).
 [7] D. S. Fisher, Phys. Rev. Lett. **56**, 416 (1985).

[8] J.C. Anglès d'Auriac, M. Preissmann and A. Seb, J. Math. and Comp. Model. **26**, 1 (1997).
 [9] H. Rieger, in: *Advances in Computer Simulation*, Ed. J. Kertesz and I. Kondor, Lecture Notes in Physics **501**, Springer, Heidelberg, 1998.
 [10] M. J. Alava, P. M. Duxbury, C. Moukarzel and H. Rieger, in Ed. C. Domb and J.L. Lebowitz, *Phase transitions and Critical Phenomena*, **18**, Academic press, New York 2001.
 [11] A.K. Hartmann and H. Rieger, *Optimization Algorithms in Physics*, Wiley-VCH, Berlin, to be published 2001.
 [12] A. A. Middleton and D. S. Fisher, unpublished.
 [13] H. Rieger, Phys. Rev B **52**, 6659 (1995); See also H. Rieger and A. P. Young, J. Phys. A **26**, 5279 (1993).
 [14] D. P. Belanger, A. R. King, V. Jaccarino and J. L. Cardy, Phys. Rev. B **28**, 2522 (1983); D. P. Belanger and Z. Slanič, J. Magn. and Magn. Mat. **186**, 65 (1998).
 [15] M. N. S. Swamy and K. Thulasiraman, *Graphs, Networks and Algorithms*, Wiley, New York 1991.
 [16] J. D. Claiborne, *Mathematical Preliminaries for Computer Networking*, Wiley, New York 1990.
 [17] W. Knödel, *Graphentheoretische Methoden und ihre Anwendung*, Springer, Berlin 1969.
 [18] K. Mehlhorn and St. Näher, *The LEDA Platform of Combinatorial and Geometric Computing*, Cambridge University Press, Cambridge 1999; see also <http://www.mpi-sb.mpg.de/LEDA/leda.html>.
 [19] J.-C. Picard and H. D. Ratliff, Networks **5**, 357 (1975).
 [20] J. L. Träff, Eur. J. Oper. Res. **89**, 564 (1996).
 [21] R. E. Tarjan, *Data Structures and Network Algorithms*, Society for Industrial and Applied Mathematics, Philadelphia 1983.
 [22] A.V. Goldberg and R.E. Tarjan, J. ACM **35**, 921 (1988).
 [23] B. Cherkassky and A. Goldberg, Algorithmica **19**, 390 (1997).
 [24] A.V. Goldberg, R. Satish, J. ACM, **45**, 783 (1998).
 [25] A.T. Ogielski, Phys. Rev. Lett. **57**, 1251 (1986).
 [26] A.K. Hartmann and U. Nowak, Eur. Phys. J. B **7**, 105 (1999).
 [27] J.-C. Anglès d'Auriac and N. Sourlas, Europhys. Lett. **39**, 473 (1997).
 [28] N. Sourlas, Comp. Phys. Comm. **121-122**, 183 (1999).
 [29] U. Nowak, K.D. Usadel and J. Esser, Physica A **250**, 1 (1998).
 [30] The RFIM with a delta-distribution of the random fields ($\pm h$) exhibits an exponential ground-state degeneracy.
 [31] J.-C. Picard and M. Queyranne, Math. Prog. Study **13**, 8 (1980).
 [32] A.K. Hartmann, Physica A **248**, 1 (1998).
 [33] S. Bastea and P.M. Duxbury, Phys. Rev. E **58**, 4261 (1998).
 [34] Actually we used more samples for some values of h than for others. Hence, for each data point, we only used realizations where the ground states were calculated at both the left and the right boundary of the corresponding interval.
 [35] B. Efron, *The Jackknife, the Bootstrap and Other Resampling Plans*, SIAM 1982.
 [36] W.H. Press, S.A. Teukolsky, W.T. Vetterling and B.P. Flannery, *Numerical Recipes in C*, Cambridge University

Press, Cambridge 1995.

- [37] We used the Levenberg-Marquardt routine described in Ref. [36].
- [38] G. Grinstein, Phys. Rev. Lett. **34** 944 (1976).
- [39] J. Villain J. Physique **46**, 1843 (1985).
- [40] M. Gofman, J. Adler, A. Aharony, A. B. Harris, and M. Schwartz, Phys. Rev. Lett. **71**, 1569 (1993).
- [41] M. Schwartz and A. Soffer, Phys. Rev. Lett. **55**, 2499 (1985).
- [42] A. Aharony, Phys. Rev B **18**, 3318 (1978).
- [43] A. Houghton, A. Khurana, and F. J. Seco, Phys. Rev B **34**, 1700 (1986); A. Houghton, A. Khurana, and F. J. Seco, Phys. Rev. Lett. **55**, 856 (1985).
- [44] V. Privman, P. C. Hohenberg, and A. Aharony, in *Phase Transitions and Critical Phenomena*, Vol. 14, Ed. C. Domb and J. L. Lebowitz, Academic Press (New York), p.1 (1991).
- [45] See for example the discussion on p. 11 of Ref. [44].
- [46] C. Bervillier Phys. Rev. B **34**, 8141 (1986).
- [47] A. A. Middleton and D. S. Fisher, cond-mat/0107489.